Determination of ^{193}Au and ^{193}Hg atomic masses by the ^{197}Au(α, ^{8}He)^{193}Au reaction

S. Kato
Department of Physics, Yamagata University, Yamagata 990, Japan

S. Kubono, M. H. Tanaka, M. Yasue, T. Nomura, Y. Fuchi, S. Ohkawa, T. Miyachi, and K. Iwata*
Institute for Nuclear Study, University of Tokyo, Tanashi 188, Japan

T. Suehiro
Tohoku Institute of Technology, Sendai 982, Japan

Y. Yoshida
Sagami Women's University, Sagamihara, Kanagawa 228, Japan
(Received 28 September 1988)

The atomic mass excess of ^{193}Au was determined to be -33.419 ± 0.011 MeV for the first time from the measured Q value of -26.919 ± 0.009 MeV for the ^{197}Au(α, ^{8}He)^{193}Au reaction. The atomic mass excess of ^{193}Hg was also determined to be -31.080 ± 0.032 MeV by using the known Q value of ^{193}Hg beta decay to ^{193}Au. These results were compared with some predicted values.

I. INTRODUCTION

The ground-state mass is undoubtedly one of the most fundamental quantities of atomic nuclei. Many authors[1–16] have been discussing it from phenomenological, macroscopic or microscopic approaches. Many of them predicted unmeasured masses of atomic nuclei by mass formulae or mass relations whose parameters were extracted from the measured ones. For an accurate prediction, and also for a deeper understanding of the nature of atomic nuclei, the addition of experimental values of masses is always valuable.

The Q value of alpha or beta decay is often used for determining atomic mass because it gives a mass relation between the parent and the daughter nuclei. The mass of an unmeasured nucleus can be calculated if its decay energy to or from the nucleus of a known mass has been measured. Masses of many neutron-rich nuclei have been determined by Q values of charged-particle emission (alpha or beta decay). On the other hand, proton-rich nuclei do not always decay through the charged-particle emission. Sometimes they decay through electron capture whose Q value is difficult to measure. Therefore, the mass relation of the proton-rich nuclei through beta decay is often disconnected. For the determination of the mass of proton-rich nuclei, other means also play important roles.

The Q value of nucleon transfer reactions connects the mass of the residual nucleus with that of the target nucleus. The (α, ^{8}He) reaction is very suitable for the mass determination because it can produce many proton-rich nuclei of unmeasured mass. Predicted reaction Q values are largely negative for lighter targets and their absolute values decrease for heavier targets. Although we expect larger reaction cross sections for lighter targets, measurements of the Q values are difficult because the magnetic rigidities of ^{8}He^{2+} particles are smaller than that of the incident beam even at the maximum available energy of the Institute for Nuclear Study SF cyclotron which we intended to use. From among the heavy elements, we selected ^{197}Au as the target because the mass of ^{193}Au had not been measured and we needed no isotope enrichment.

In Fig. 1, we show a mass relation among the members of the $A=193$ isobar. Nuclei of known masses are shown by bold lines. Arrows indicate that Q values of alpha or beta decay have been measured. The masses of nuclei which are connected with nuclei of known masses by the measured decay are also known. ^{193}Os, ^{193}Ir, and ^{193}Pt are connected with one another and constitute a group of known masses at the valley of the beta-stability line. Alpha decays involving ^{193}Pb, ^{193}Bi, and ^{193}Po nuclei do not connect them with any known-mass nuclei. ^{193}Tl is connected with its alpha-decay parent nucleus whose mass is known. ^{193}Au and ^{193}Hg are connected with each other, but they are isolated from other nuclei because the beta decay connecting with the next members of the $A=193$ isobar proceed through electron capture. The (α, ^{8}He) reaction can connect such isolated nuclei with target nuclei of known masses. We can determine the masses of both ^{193}Au and ^{193}Hg by measuring the Q value of the ^{197}Au(α, ^{8}He)^{193}Au reaction.

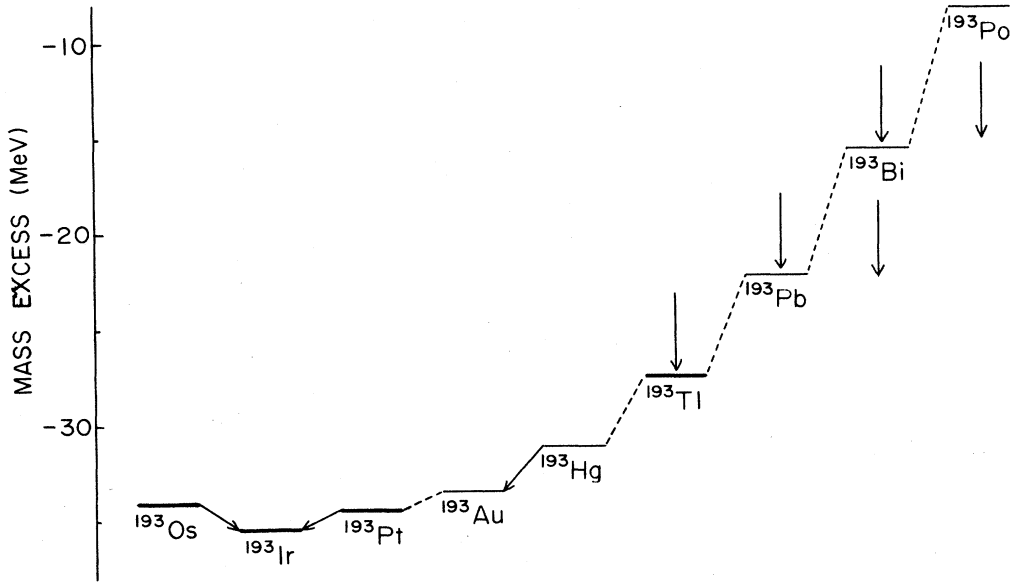

FIG. 1. A mass relation among the members of the $A = 193$ isobar. Nuclei whose masses have been measured are shown by bold lines. Arrows mean that Q values of alpha or beta decay have been measured. These Q values give the mass relations between the parent and the daughter nuclei. Broken lines mean that the Q values have not yet been measured.

II. EXPERIMENTAL PROCEDURES AND RESULTS

A. Experimental setup and data taking

We bombarded a self-supporting 1.0-mg/cm^2 thick foil of gold with a ^{4}He beam from the sector-focusing cyclotron of the Institute of Nuclear Study, University of Tokyo. The bombarding energy was 65.119 MeV. Reaction products were analyzed by a quadrupole-dipole-dipole (QDD) magnetic spectrometer[17] which was set at 8 deg from the beam direction with a slit aperture of 5 msr, and they were detected by a small detector system with the enhanced capability of particle identification.

The detector system consisted of three drift-type proportional counters and an energy counter. Primary charges drifted vertically by an imposed electric field. The fundamental structure of these proportional counters was the same as the counter in common use[18] with the spectrometer. Nichrome wires were used at the first and the third proportional counters for position measurement. We measured the position of particles twice in order to reconstruct their trajectories. The position difference information obtained from the two counters was useful for eliminating particles of improper incident angles. The position was calculated by a computer. The second proportional counter was an ordinary energy-loss counter.

The energy counter was a homemade, large silicon detector (12 cm of length, 2 mm of thickness).[19] It was set inside the gas chamber. Although the proportional counters had lengths of 21 cm, we confined the counter system to 11 cm by a metallic cover. Although the angle between trajectories of particles and the focal plane was not 90 deg, we set these counters perpendicular in order to cover a range of magnetic rigidity as broad as possible, and in order to avoid the degradation of position resolution by an off-normal incidence of particles to the counter.

The time intervals between the fast signals from the silicon detector and the energy-loss signals from vertically drifted charges provided us with information on the vertical positions on the focal plane.

The time of flight (TOF) through the magnetic spectrometer whose path length was about 7 m was obtained by the time intervals between the rf signals from the cyclotron oscillator and the fast signals from the silicon detector.

The four signals from both sides of the two position counters, the energy loss signal, the energy signal, the vertical position signal, and the TOF signal were analyzed by analog-to-digital converters. A rough hardware discrimination by the energy-loss signals was made in order to reduce the number of unnecessary events. The eightfold coincident events were recorded on magnetic tape event by event. The number of recorded events exceeded 600 000.

B. Particle identification

Figure 2 shows a contour plot of a two-dimensional spectrum of energy (abscissa) and energy loss (ordinate). For a fixed magnetic rigidity, namely after a momentum

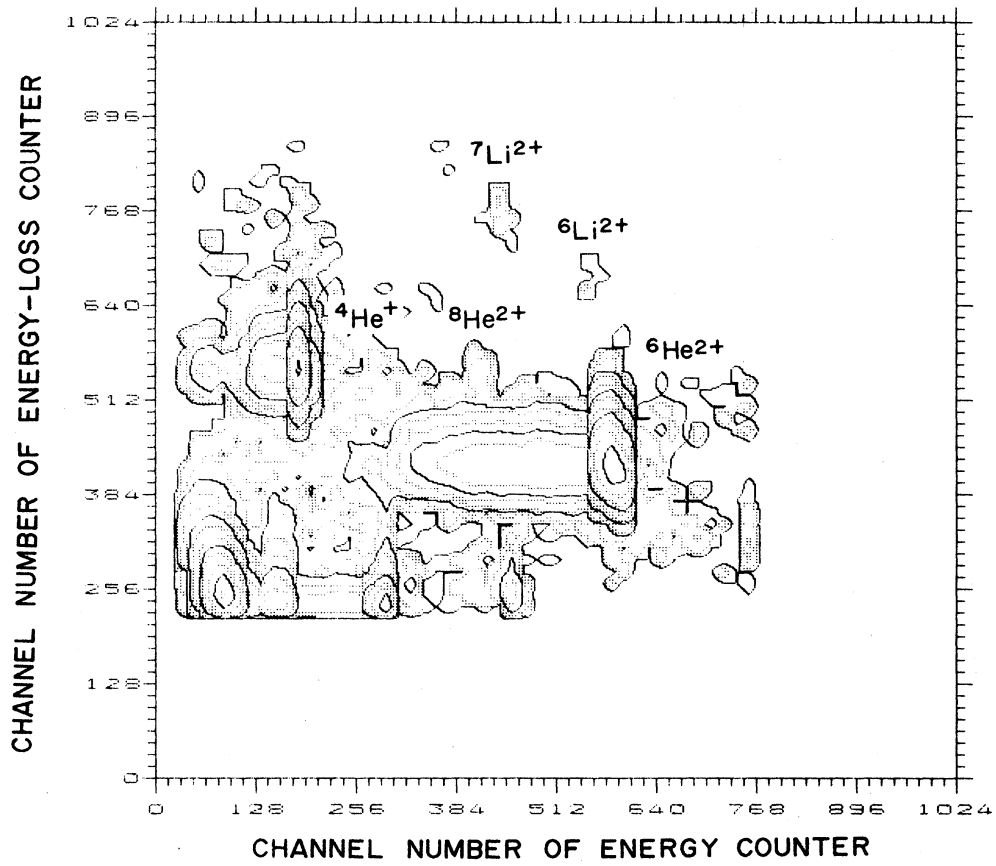

FIG. 2. A Contour plot of the two-dimensional energy (abscissa) and energy-loss (ordinate) spectrum. Although the full channel numbers are indicated by 1024×1024 channels, they have been reduced to 64×64 channels. The contour levels are in logarithmic steps. The solid contours are of 1, 10, 100, 1000, or 10 000 counts. Multiples of 2 and 5 of them are shown by dotted contours. The peak of $^{8}He^{2+}$ is expected to appear to the right of that of $^{4}He^{+}$. We could not assign particle species to the two peaks at the lower-left corner. They were later eliminated by the position difference condition.

analysis, energy and energy loss are proportional to Q^2/A and $(AZ/Q)^2$, where Q, A, and Z are the charge, mass number, and atomic number of the particles, respectively. Because the energy loss of $^{4}He^{+}$ is the same as that of $^{8}He^{2+}$, the former provided us with a convenient guide to search for the peak of the latter. Since the peak of $^{8}He^{2+}$ is not isolated enough from other particles, we had to reduce the background by the information on the position difference, the vertical position, and the TOF.

Figure 3 shows a background-reduced scatter plot of the two-dimensional spectrum of the energy (abscissa) and the position along the first position counter (ordinate). The locus of $^{8}He^{2+}$ is clearly seen. The low-lying discrete states of residual nuclei are seen for ejectiles of both $^{8}He^{2+}$ and $^{6}He^{2+}$.

Figure 4 shows the position (momentum) spectrum of $^{8}He^{2+}$ particles. Here, the position indicates the point where each trajectory intersects the focal plane. The number of counts corresponding to the ground state of ^{193}Au was 52. The cross section was obtained to be 16 nb/sr. The FWHM energy resolution of the peak was 60 keV. Most of the spread was attributed to the difference of the energy loss between ^{8}He and ^{4}He particles in the target foil.

C. Energy calibration and precision

In Fig. 3, we can see some peaks corresponding to the low-lying state of ^{195}Au on the locus of the $^{6}He^{2+}$ particles. Ten levels from ground to 1.0680 MeV excited states[20] which had been observed by the $^{197}Au(p,t)^{195}Au$ reaction were identified and were adopted as the calibration points. Their excitation energies were known with precision better than 1 keV. From a kinematical calculation which included energy-loss effect in the target, we obtained a relation between orbit radius in the spectrometer and position along the focal plane. The calibration points were fitted by second-order polynomials. The standard deviation of the calibration points from the fitted curve was 0.01 cm of radius, whose effect on the reaction Q value was 2 keV. We can regard this uncertainty as including both peak position determinations for the calibration spectrum and those of the known excitation energies.

The peaks in Fig. 4 were compared with the known excitation energies.[21] We identified the largest peak (indicated as 0.000 MeV) not with the first excited 38 keV state, but with the ground state of ^{193}Au taking into account the energy separation from the well-isolated peak

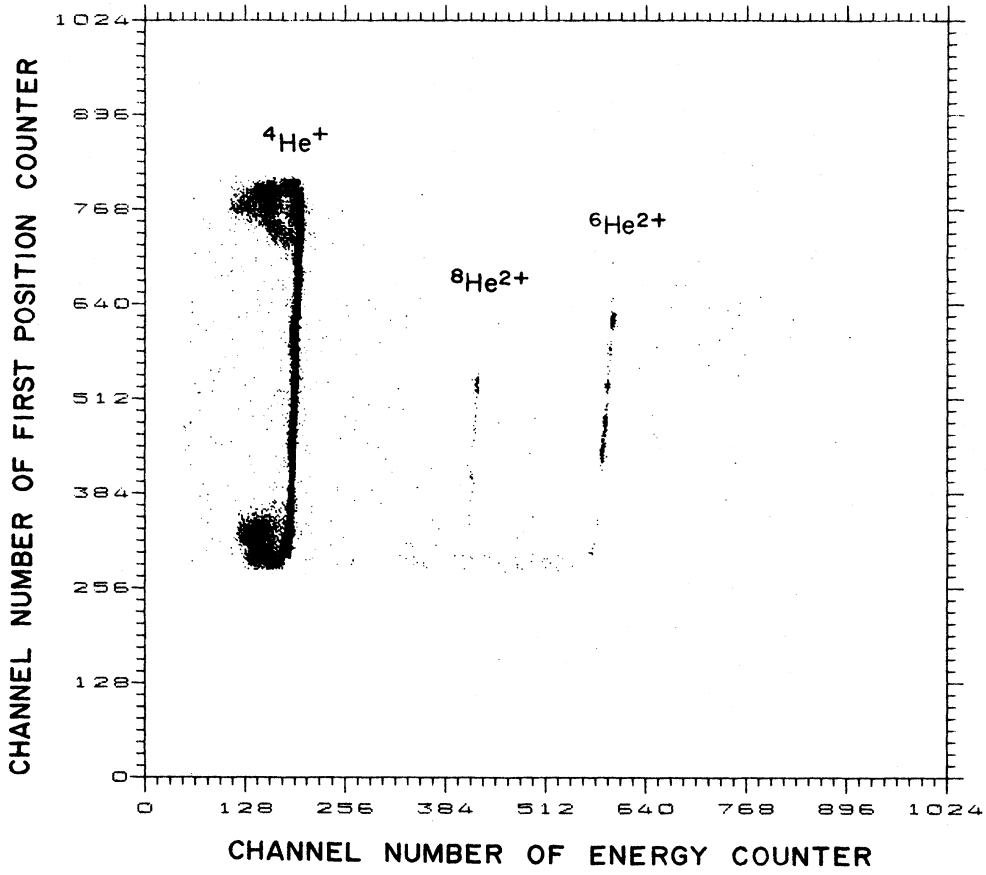

FIG. 3. A scatter plot of the two-dimensional spectrum of energy (abscissa) and position along the first counter (ordinate). We can see that low-energy tails of energy signals seen in Fig. 2 were generated at the ends of the silicon detector.

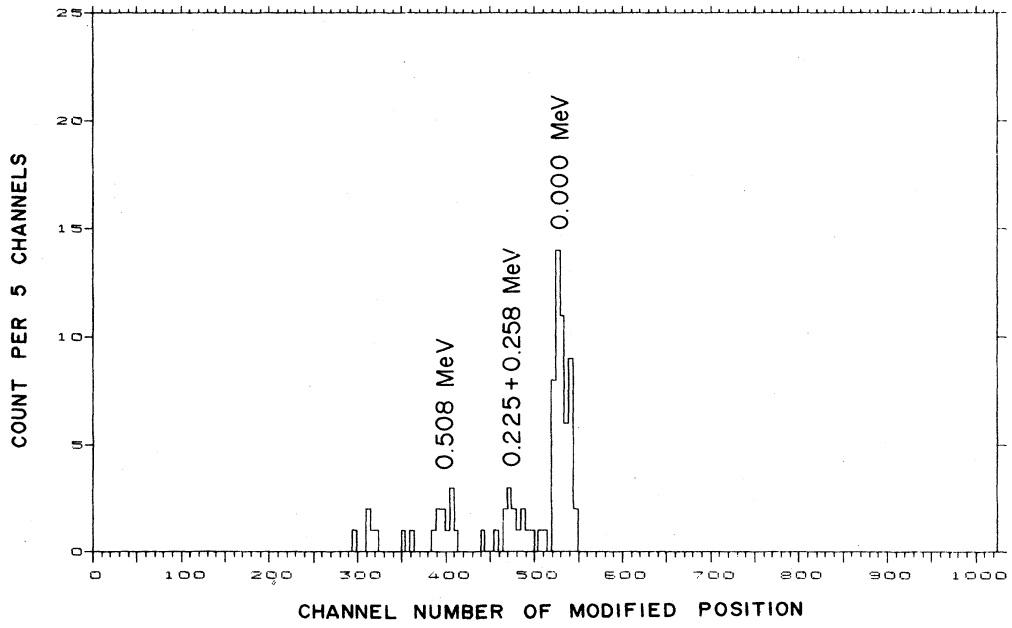

FIG. 4. Position (momentum) spectrum of the reaction ^{197}Au(α,^{8}He)^{193}Au. Indicated excitation energy values were taken from Ref. 21. The fourth peak cannot be assigned as an excited state of ^{193}Au. It is a low-energy tail of ^{6}He^{2+} at the lower momentum end of the silicon detector.

of the 0.508-MeV excited state. From the momentum spectrum and the calibration, we obtained the ground-state Q value of -26.919 MeV.

The channel number of the peak position was determined with a precision of ± 0.9 channel. This uncertainty corresponded to ± 4 keV of the Q value.

The uncertainties of the known mass excesses[5] of nuclei ^{197}Au, ^{195}Au, ^{6}He, and ^{4}He had to be taken into account because we utilized the Q value of the ^{197}Au(α,^{6}He)^{195}Au reaction for the calibration. The quantities of the first three were ± 4 keV, ± 4 keV, and ± 1 keV, respectively. That of ^{4}He was negligible.

The uncertainty of the incident energy was estimated to be ± 23 keV, which was attributed to a slit aperture of 5 mm of the beam-analyzing system. Because we measured ^{8}He and ^{6}He simultaneously, the uncertainty of the incident energy resulted in only a small effect on the reaction Q value (± 4 keV).

Nominal thickness of the target foil was 1.0 mg/cm^2, whose uncertainty of the thickness was smaller than 0.1 mg/cm^2. Although most of the peak spread in the momentum spectrum of Fig. 4 was attributed to the energy-loss difference between ^{8}He and ^{4}He particles in the target, the effect of the uncertainty of the target thickness on the Q value was found to be small (± 2 keV).

The angle of incidence to the focal plane was known to be about 35 deg.[17] It changes by ± 5 deg at both ends of the focal plane. Even if the focal plane were rotated by 5 deg, the resultant Q value change would be smaller than 1 keV.

TABLE I. Origins and their quantities contributing to the uncertainty of the Q value of the ^{197}Au(α,^{8}He)^{193}Au reaction.

Uncertainty of	Effect on the Q value (keV)
Peak position	4
Mass of ^{197}Au	4
Mass of ^{195}Au	4
Mass of ^{6}He	1
Calibration points	2
Incident energy	4
Target thickness	2
Focal plane angle	1
Total	9

The origins of the uncertainties of the reaction Q value were summarized in Table I. The total uncertainty amounted to ± 9 keV.

III. DISCUSSION

From the Q value of -26.919 ± 0.009 MeV for the ^{197}Au(α,^{8}He)^{193}Au reaction and the mass excess of 31.598 ± 0.007 MeV (Ref. 5) for ^{8}He, we obtained -33.419 ± 0.011 MeV for the mass excess of ^{193}Au. The uncertainty of mass excess of ^{8}He was larger than any other uncertainties listed in Table I. By an improvement in the mass excess of ^{8}He in the future, that of ^{193}Au will be automatically improved.

TABLE II. A comparison of the measurement and the predictions of mass excesses of ^{193}Au and ^{193}Hg.

Authors	Mass excess (MeV) ^{193}Au	^{193}Hg
Experiment		
present	-33.419 ± 0.011	-31.080 ± 0.032
Predictions		
Garvey *et al.*[a]	-33.36	-30.85
Uno-Yamada (constant)[b]	-33.056 ± 0.541	-30.898 ± 0.593
Uno-Yamada (linear)[b]	-33.447 ± 0.111	-30.948 ± 0.441
Dussel-Caurier-Zuker[c]	-33.60	-30.97
Möller-Nix[d]	-33.65	-30.95
Möller *et al.*[e]	-33.34	-30.81
Comay-Kelson-Zidon[f]	-33.58 ± 0.67	-31.30 ± 0.63
Satpathy-Nayak[g]	-33.72	-31.11
Tachibana *et al.*[h]	-33.10	-30.94
Spanier-Johannson[i]	-33.50	-31.79
Jänecke-Masson[j]	-33.25	-31.05
Masson-Jänecke[k]	-33.44	-31.13
Wapstra *et al.* (1977)[l]	-33.360 ± 1.000	-31.020 ± 1.000
Wapstra *et al.* (1983)[m]	-33.490 ± 0.100	-31.150 ± 0.100
Wapstra *et al.* (1986)[n]	-33.430 ± 0.100	-31.090 ± 0.100

[a]Reference 1.
[b]Reference 2.
[c]Reference 8.
[d]Reference 9.
[e]Reference 10.
[f]Reference 11.
[g]Reference 12.
[h]Reference 13.
[i]Reference 14.
[j]Reference 15.
[k]Reference 16.
[l]Reference 3.
[m]Reference 4.
[n]Reference 5.

The beta-decay Q value (expressed as that of electron capture) directly gives the difference of atomic masses between the parent and the daughter nuclei. Since the Q value of ^{193}Hg decay had been known to be 2.339 ± 0.030 MeV,[22,23] we derived -31.080 ± 0.032 MeV for the mass excess of ^{193}Hg.

The atomic masses of ^{193}Au and ^{193}Hg were obtained for the first time here. In Table II, we compared them with some predicted masses. The latter values are distributed around the measured ones. They are in agreement within the indicated errors.

In the mass calculation by Uno-Yamada, the parameters for the shell effect change according to the proton and neutron numbers. The number of parameters for each proton or neutron number is one for "constant shell," and two for "linear shell" calculations. It is natural that the latter model predicted better values.

The predicted values by Wapstra *et al.* agree with the present values very well. In their list of mass excess,[4,5] masses of the next $A=193$ isobar were known. The reason for the good agreement with the data could be that they interpolated the known values. It is interesting to note that the estimated values by these authors were oscillating and converging to the present values each time they revised them.

IV. SUMMARY

We measured the Q value of the ^{197}Au(α,^{8}He)^{193}Au reaction. From the Q value of -26.919 ± 0.009 MeV, we determined the ^{193}Au atomic mass excess to be -33.419 ± 0.011 MeV for the first time. We also obtained the mass excess of -31.080 ± 0.032 MeV for ^{193}Hg from the known beta-decay Q value. The measured values were in good agreement with the predicted values.

The authors are grateful to members of maintenance group of the Institute for Nuclear Study SF cyclotron for their operation of the accelerator.

---

*Present address: College of General Education, University of Tokyo, Japan.

[1]G. T. Garvey, W. J. Gerace, R. L. Jaffe, I. Talmi, and I. Kelson Rev. Mod. Phys. **41**, S1 (1969).
[2]M. Uno and M. Yamada, Institute for Nuclear Study, University of Tokyo, Report INS-NUMA-40, 1982.
[3]A. H. Wapstra and K. Bos, At. Data Nucl. Data Tables **19**, 177 (1977).
[4]A. H. Wapstra and G. Audi, Nucl. Phys. **A432**, 1 (1985).
[5]A. H. Wapstra, G. Audi, and R. Hoekstra, At. Data Nucl. Data Tables, **39**, 281 (1988).
[6]P. E. Haustein, At. Data Nucl. Data Tables **39**, 185 (1988).
[7]A. Pape and M. S. Antomy, At. Data Nucl. Data Tables **39**, 201 (1988).
[8]G. Dussel, E. Caurier, and A. P. Zuker, At. Data Nucl. Data Tables **39**, 205 (1988).
[9]P. Möller and J. R. Nix, At. Data Nucl. Data Tables **39**, 213 (1988).
[10]P. Möller, W. D. Myers, W. J. Swiatecki, and J. Treiner, At. Data Nucl. Data Tables **39**, 225 (1988).
[11]E. Comay I. Kelson, and A. Zidon, At. Data Nucl. Data Tables **39**, 235 (1988).
[12]L. Satpathy and R. C. Nayak, At. Data Nucl. Data Tables **39**, 241 (1988).
[13]T. Tachibana, M. Uno, M. Yamada, and S. Yamada, At. Data Nucl. Data Tables **39**, 251 (1988).
[14]L. Spanier and S. A. E. Johansson, At. Data Nucl. Data Tables **39**, 259 (1988).
[15]J. Jänecke and P. J. Masson, At. Data Nucl. Data Tables **39**, 265 (1988).
[16]P. J. Masson and J. Jänecke, At. Data Nucl. Data Tables **39**, 273 (1988).
[17]S. Kato, T. Hasegawa, and M. Tanaka, Nucl. Instrum. Methods **154**, 19 (1978).
[18]M. H. Tanaka, S. Kubono, and S. Kato, Nucl. Instrum. Methods **195**, 509 (1982).
[19]T. Miyachi, S. Ohkawa, T. Emura, M. Nishimura, O. Nitoh, K. Takahashi, S. Kitamura, Y. Kim, T. Abe, and H. Matsuzawa, Jpn. J. Appl. Phys. **27**, 307 (1988).
[20]*Table of Isotopes,* 7th ed., edited by C. M. Lederer and V. S. Shirley (Wiley, New York, 1978), pp. 1254 and 1255.
[21]See Ref. 20, pp. 1239–1241.
[22]*Table of Radioactive Isotopes,* edited by V. S. Shirley (Wiley, New York, 1986), p. 193.
[23]A. H. Wapstra, G. Audi, and R. Hoeksetra, Nucl. Phys. **A432**, 185 (1985).